ENERGY DEPENDENCE OF SPIN–SPIN FORCES IN 90°_{cm} ELASTIC p–p SCATTERING ☆

A. LIN
Abadan Institute of Technology, Abadan, Iran

J.R. O'FALLON [1], L.G. RATNER and P.F. SCHULTZ
Argonne Universities Association and Argonne National Laboratory, Argonne, IL 60439, USA

K. ABE [2], D.G. CRABB, R.C. FERNOW, A.D. KRISCH, A.J. SALTHOUSE, B. SANDLER and K.M. TERWILLIGER
Randall Laboratory of Physics, The University of Michigan, Ann Arbor, MI 48109, USA

Received 31 January 1978

We measured $d\sigma/dt(90^\circ_{cm})$ for $p\uparrow + p\uparrow \to p + p$ from 1.75 to 5.5 GeV/c, using the Argonne zero-gradient synchrotron 70% polarized proton beam and a 70% polarized proton target. We found that the spin–spin correlation parameter, A_{nn}, equals 60% at low energy, then drops sharply to about 10% near 3.5 GeV/c, and remains constant up to 5.5 GeV/c.

Measuring the fixed-angle energy dependence of proton–proton elastic scattering at 90°_{cm} is a sensitive way to probe the short-range behavior of strong interactions [1,2]. For $p + p \to p + p$, 90°_{cm} is a special symmetry point where the pure-spin cross sections may be especially important. The spin dependence of high-energy p–p scattering was first successfully studied in polarized target experiments at Berkeley [3], CERN [4], and Argonne [5]. The Argonne zero-gradient synchrotron (ZGS) polarized proton beam (PPB) allows precise measurements [6–12] of the spin–spin interactions, which is parameterized by A_{nn}, the spin–spin correlation parameter ‡1. We recently studied the fixed-angle energy dependence of A_{nn} at 90°_{cm} using the ZGS PPB and our polarized proton target (PPT). We found a sharp change in $A_{nn}(90^\circ_{cm})$ near 3.5 GeV/c.

The momentum of the ZGS polarized beam was varied between 1.75 and 5.5 GeV/c. Care was taken to avoid momenta very close to known depolarizing resonances. At each momentum the beam polarization, P_b, was maximized by the ZGS staff [14] using the fast uncalibrated CERN polarimeter [15] to tune through each resonance below extraction energy. When the polarization was maximum the left–right asymmetry was measured using the beam-1 elastic polarimeter [6,15] shown in fig. 1. The beam polarization was then calculated using

$$P_b = (1/A)[(L - R)/(L + R)]. \qquad (1)$$

A is the analyzing power for $p + p \to p + p$ at $-t = 0.5$ $(\mathrm{GeV}/c)^2$ where our polarimeter was set at each incident momentum. The value of A was first obtained by averaging previously measured values of A [3–5,7] at nearby $-t$ and P_{lab} values. Using these average values we sometimes obtained P_b larger than 100%; we thus concluded that there were errors in some of the previous measurements of A. It was not possible to measure A at $-t = 0.5$ $(\mathrm{GeV}/c)^2$ with our polarized target without major changes in the downstream spectrometer in fig. 1.

We therefore decided to determine P_b with the 50 MeV polarimeter [6,15] at the end of the LINAC just

☆ Work supported in part by the Department of Energy.
[1] On leave from the Department of Physics, St. Louis University, St. Louis, MO 63103.
[2] Present address: Department of Physics, University of California, Los Angeles, CA 90024.
‡1 The spin–spin correlation parameter, previously denoted C_{nn}, is now denoted A_{nn} according to the new Ann Arbor convention [13].

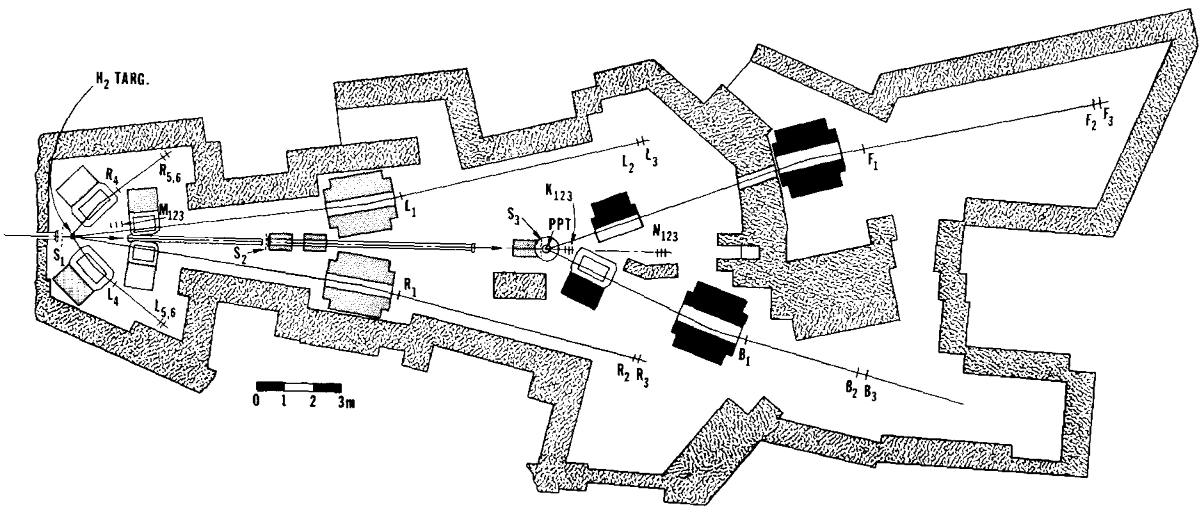

Fig. 1. Layout of the experiment. The polarized beam passes through the liquid-H_2 target and its polarization is measured by comparing the number of elastic events seen in the L and R spectrometers of the polarimeter. The beam then scatters in the polarized proton target (PPT) and the elastic events are counted by the F and B counters. The M, N, and K counters are intensity monitors, while S_1, S_2 and S_3 monitor the beam position, size, and angle.

before injection into the ZGS. This measured p-carbon elastic scattering at 55° in the lab where the analyzing power is 88 ± 5%. This polarimeter has been cross-calibrated [8–12] against the beam-1 polarimeter at 6 and 11.75 GeV/c where the p + p → p + p analyzing power is very well measured. The 50 MeV measurement of P_b clearly gives an upper limit on the polarization, and thus a lower limit on A, since the polarization cannot increase during acceleration. P_b could, of course, decrease. However the resonance-jumping correction magnets [15] were frequently retuned at each depolarizing resonance below the extraction momentum and no significant depolarization was found [14]. Thus we believe that, when it was properly maximized, P_b at extraction energy was equal to P_b at 50 MeV within ±3%. Therefore we used the beam-1 polarimeter measurements of $(L - R)/(L + R)$ at each extraction momentum to obtain the analyzing power for p + p → p + p at $-t = 0.5$ (GeV/c)^2. These values of A are given in table 1 along with our estimated experimental errors. They agree with some earlier results [3,7] but disagree with others [4,5]. We used the values of A in table 1 to obtain P_b for our long data runs when P_b was possibly not maximized. Our average value of P_b for these measurements of $A_{nn}(90^\circ_{cm})$ was about 70% with a relative error of ±4.3% point to point and ±5.7% normalization.

We scattered the polarized proton beam from the Michigan–Argonne polarized proton target PPT-V [8–12,16,17] of ethylene glycol doped with $K_2Cr_2O_7$. We measured the target polarization, P_t, which averaged about 70%, with two independent NMR coils [10], with a precision of about ±3%.

The double-armed FB spectrometer in fig. 1 detected events when the polarized proton beam elastically scattered from the polarized proton target at 90°_{cm}. This

Table 1
Measurements of the analyzing power for p + p → p + p near $-t = 0.5$ (GeV/c)^2 for different values of incident momentum. The statistical errors are always less than 0.1%. The quoted errors are due to our estimated ±4.3% relative systematic error in P_b. There is an additional normalization error of ±5.7% of A, caused by the uncertainty in $A_{p\text{-}C}$.

P_{lab} (GeV/c)	$-t$ (GeV/c)^2	A (%)
1.75	0.18	44.0 ± 1.9
2.50	0.36	33.0 ± 1.4
3.10	0.50	25.4 ± 1.1
3.50	0.50	21.9 ± 0.9
4.00	0.50	18.3 ± 0.8
4.40	0.50	15.6 ± 0.7
5.00	0.50	13.4 ± 0.6
5.50	0.50	12.2 ± 0.5

Table 2
Measurements of A and A_{nn} for 90°_{cm} p + p → p + p for various values of incident lab momentum. The quoted errors include statistical errors and the systematic error mostly due to the uncertainty in P_b. There is an additional normalization error of ±7.2% of the value of A_{nn} which is primarily due to the normalization uncertainties in P_b and P_t and the teflon subtraction.

P_{lab} (GeV/c)	A (%)	A_{nn} (%)
1.75	−0.1 ± 0.6	59.7 ± 2.6
2.50	0.0 ± 0.3	57.2 ± 2.5
3.10	2.1 ± 0.4	47.4 ± 2.1
3.50	0.3 ± 0.4	31.6 ± 1.5
4.00	0.0 ± 0.4	11.9 ± 0.8
4.40	1.5 ± 0.6	9.1 ± 1.5
5.00	−0.3 ± 0.5	10.6 ± 0.8
5.50	−1.1 ± 0.6	9.6 ± 1.2

spectrometer contained four magnets and the $F_1F_2F_3$ and $B_1B_2B_3$ scintillation counters and measured the angle and momentum of both outgoing protons. The PPT magnet field of 10.67 kG m bent both outgoing protons to the right. By varying the magnet currents we covered the range P_{lab} = 1.75 → 5.5 GeV/c without moving the detectors. The 15 × 20 cm^2 F_3 counter defined the center-of-mass solid angle of $\sim 10^{-3}$ sr. The momentum bite was typically $\Delta P/P = \pm 7\%$. The B counters were over-matched to allow for beam size and divergence, magnet variations, and multiple Coulomb scattering. The accidentals were typically 0.2% and were continuously monitored and subtracted. Recoil magnet curves and teflon bead runs measured the non-hydrogen event rate, which was 3 ± 1% near 1.75 and 5.5 GeV/c. Thus a 3 ± 1% subtraction was made at each P_{lab}.

The relative beam intensity at the PPT, I_0, was monitored by the scintillation telescopes, M, N, and K [‡2]. The beam size at the 29 mm diameter by 41 mm long PPT was about 14 mm full width at half maximum and the beam movement was less than 0.5 mm. More than 95% of the beam passed through the PPT. Possible systematic errors due to variations in this number were reduced to below 1% by reversing the beam spin every pulse and the target spin every 6 h.

We obtained the four normalized elastic event rates,

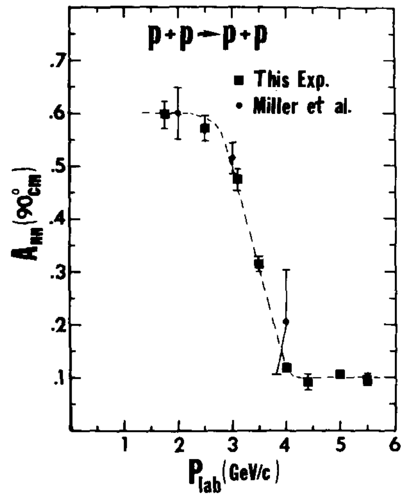

Fig. 2. The spin–spin correlation parameter, A_{nn}, for p–p elastic scattering at 90° in the center-of-mass is plotted against the incident lab momentum, along with earlier measurements [7]. The curves are hand-drawn lines to guide the eye.

$$N_{ij} = E(ij)/I_0(ij), \tag{2}$$

by simultaneously measuring the number of elastic events $E(ij)$ and the number of incident protons $I_0(ij)$ in each of the four initial spin states ($ij \equiv$ beam, target = ↑↑, ↑↓, ↓↑, or ↓↓). Both spins were measured normal to the horizontal scattering plane. The spin–spin correlation parameter, A_{nn}, and the spin–orbit analyzing power, A, obtained from the equations

$$A_{nn} = \frac{N_{\uparrow\uparrow} - N_{\uparrow\downarrow} - N_{\downarrow\uparrow} + N_{\downarrow\downarrow}}{P_b P_t \Sigma N_{ij}}, \qquad A = \frac{2(N_{\uparrow\uparrow} - N_{\downarrow\downarrow})}{(P_b + P_t)\,\Sigma N_{ij}}, \tag{3}$$

are listed in table 2 along with their estimated errors. Because of symmetry, A at 90°_{cm} must be zero. This constraint was typically satisfied within ±1%. The values of A_{nn} are plotted in fig. 2 against P_{lab}. We obtained the two independent pure two-spin cross sections at 90°_{cm} from the equations

$$(\mathrm{d}\sigma/\mathrm{d}t)_{\uparrow\uparrow} = (\mathrm{d}\sigma/\mathrm{d}t)_{\downarrow\downarrow} = \langle \mathrm{d}\sigma/\mathrm{d}t\rangle(1 + A_{nn}), \qquad (\mathrm{d}\sigma/\mathrm{d}t)_{\uparrow\downarrow} = (\mathrm{d}\sigma/\mathrm{d}t)_{\downarrow\uparrow} = \langle \mathrm{d}\sigma/\mathrm{d}t\rangle(1 - A_{nn}). \tag{4}$$

The spin-average p + p → p + p cross section, $\langle \mathrm{d}\sigma/\mathrm{d}t\rangle$, was taken from the 90° measurements of Kammerud et al. [2] and Akerlof et al. [1].

[‡2] Our results are totally independent of the ±7% normalization error in the calibration of I_0 with foil irradiations.

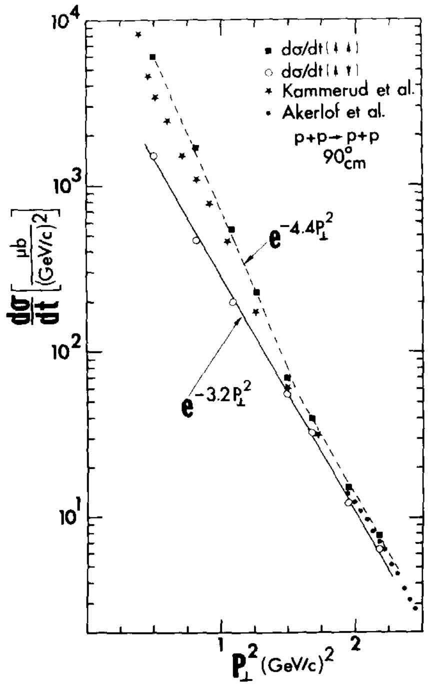

Fig. 3. The two independent pure-initial-spin differential cross sections $(d\sigma/dt)_{\uparrow\uparrow}$ and $(d\sigma/dt)_{\uparrow\downarrow}$ for p–p elastic scattering at 90° in the center-of-mass are plotted against $P_\perp^2$ as the incident P_{lab} is varied. The initial spins are measured normal to the scattering plane. These pure-spin cross sections are normalized to measurements [1,2] of $\langle d\sigma/dt \rangle$ which are also plotted.

The spin–spin correlation parameter, A_{nn}, measures the spin–spin interaction since it parameterizes the difference between the spin-parallel and spin-antiparallel cross sections. In fig. 2 the sharp change in $A_{nn}(90^\circ_{cm})$ near $P_{lab} = 3.5$ GeV/c is very clear. At low energy A_{nn} is approximately 60% which implies that $(d\sigma/dt)_{\uparrow\uparrow}$ is some 4 times larger than $(d\sigma/dt)_{\uparrow\downarrow}$. Throughout the range $P_{lab} = 4.0 \to 5.5$ GeV/c, A_{nn} is equal to 10% within the 1% errors. Thus the strength of the spin–spin interaction shifts rapidly from a 60% level to a 10% level. This shift may suggest a change of the 90°_{cm} scattering mechanism for p + p → p + p, near 3.5 GeV/c.

One can perhaps see this effect more clearly in fig. 3, where the pure-spin cross sections are plotted against $P_\perp^2$ showing the 90°_{cm} fixed-angle energy dependence of $p_\uparrow + p_\uparrow \to p + p$. This gives an overall view of the spin dependence at 90°_{cm} which is a special symmetry point for p–p elastic scattering. The spin-averaged 90°_{cm} cross section $\langle d\sigma/dt \rangle$ is also shown [1,2]. Notice that $(d\sigma/dt)_{\uparrow\downarrow}$ has a single $\exp(-3.2P_\perp^2)$ component which extends down to $P_\perp^2 = 0.5$ (GeV/c)^2 where the "diffraction" region begins. However $(d\sigma/dt)_{\uparrow\uparrow}$ has an additional $\exp(-4.4P_\perp^2)$ component extending from the "diffraction" region up to $P_\perp^2 = 1.5$ (GeV/c)^2. Kammerud et al. [2] suggested the existence of such a component in p–p elastic scattering on the basis of their spin-average measurements at 90°_{cm}. It appears that this component only occurs in the triplet state and can therefore be seen much more clearly in our pure spin state experiment. We do not understand the theoretical reason for this triplet component.

We are very grateful to the ZGS staff for the continued improvement of the polarized beam and to J.A. Bywater for his help operating PPT-V. We would like to thank J. Hauser, H.F. Sklar and M.J. Yatchman for their help in running.

References

[1] C.W. Akerlof et al., Phys. Rev. 159 (1967) 1138.
[2] R.C. Kammerud et al., Phys. Rev. D4 (1971) 1309.
[3] P. Grannis et al., Phys. Rev. 148 (1966) 1297.
[4] M. Borghini et al., Phys. Lett. 24B (1967) 77;
M. Borghini et al., Phys. Lett. 31B (1970) 405;
M. Borghini et al., Phys. Lett. 36B (1971) 501;
M.G. Albrow et al., Nucl. Phys. B23 (1970) 445.
[5] N.E. Booth et al., Phys. Rev. Lett. 21 (1968) 651; 23 (1969) 192;
D.J. Sherden et al., Phys. Rev. Lett. 25 (1970) 898;
J.H. Parry et al., Phys. Rev. D8 (1973) 45.
[6] E.F. Parker et al., Phys. Rev. Lett. 31 (1973) 783;
J.R. O'Fallon et al., Phys. Rev. Lett. 32 (1974) 77;
W. de Boer et al., Phys. Rev. Lett. 34 (1975) 558.
[7] G. Hicks et al., Phys. Rev. D12 (1975) 2594;
D.H. Miller et al., Phys. Rev. Lett. 36 (1976) 763;
I.P. Auer et al., Phys. Rev. Lett. 37 (1976) 1727.
[8] R.C. Fernow et al., Phys. Lett. 52B (1974) 243.
[9] L.G. Ratner et al., Phys. Rev. D15 (1977) 604.
[10] K. Abe et al., Phys. Lett. 63B (1976) 239.
[11] H.E. Miettinen et al., Phys. Rev. D16 (1977) 549.
[12] J.R. O'Fallon et al., Phys. Rev. Lett. 39 (1977) 733.
[13] AIP Conf. Proc. (1978), to be published.
[14] L.G. Ratner et al., private communication.
[15] T. Khoe et al., Particle Accelerators 6 (1975) 213.
[16] J.A. Bywater, R.C. Fernow and S.W. Gray, ANL Internal Report (1975) unpublished.
[17] M. Borghini et al., unpublished.